

# LIVE LOAD DISTRIBUTION FACTORS FOR HORIZONTALLY CURVED CONCRETE BOX GIRDER BRIDGES

Mandeep<sup>1</sup>, Er. Sandeep Pannu <sup>2</sup>(Asst. Prof.)

DEPARTMENT OF CIVIL ENGINEERING MATU RAM INSTITUTE OF ENGINEERING

&MANAGEMENT<sup>1,2</sup>, ROHTAK HARYANA

\*\*\*

**Abstract** -The paper presents the effect of curvature on horizontally curved single cell box girder concrete bridge deck for various degrees of curvature such as 15°, 30° and 45°. The end supports are provides as simply supports. For this study the models have been prepared by using finite element method in the CSi Bridge software. The response of the parameters such as shear force, bending moment, and torsion under the dead load and live load (70R Wheel IRC Loading) is studied.

**Key-Words:** Curved box girder bridge decks, pressures concrete, finite element model in Csi Bridge.

## 1. INTRODUCTION

The live burden dissemination factors (LLDF) portrayed in the AASHTO-LFD determinations had been utilized for over 50 years preceding their update in the AASHTO-LRFD Bridge Design Specification. The recipes spoke to in AASHTO-LFD depend on the brace dividing just and are normally introduced as S/D, where S is the separating and D is a steady dependent on the scaffold type. This strategy is fit to straight and non-slanted extensions as it were. While the recipes spoke to in AASHTO-LRFD are progressively helpful and exact since they consider more boundaries, for example, connect length, chunk thickness, and number of cells for the crate support connect typ. The change in AASHTO-LRFD conditions has created some enthusiasm for the scaffold designing world and has brought up certain issues. Slanted Bridges will be picked up by utilizing AASHTO-LRFD Specification [3] Since 1931, live load distribution factors have been described in the Standard Specification for Highway Bridges. The early values have been updated and modified in 1930 by Westergaard and in 1948 by Newmark as new research results became available. The distribution factor presented in AASHTO Standard Specifications was S/5.5 for a bridge constructed with a concrete deck supported on pre-stressed concrete girders. This is applicable for bridges that carry two or more lanes of traffic, where S is the girder spacing in feet. This factor is applied to the moment caused by one line of wheels. Even so, some researchers such as Zokaie have noted that the changes in LLDF over the last 55 years have led to inconsistencies in the load distribution criteria in the Standard Specifications these include: inconsistent changes in distribution factors to reflect changes in design

lane width; inconsistent consideration of a reduction in load intensity for multiple lane loading; and inconsistent verification of accuracy of wheel load distribution factors for various bridges [4].

## 2. Objective of the Study

The target of this examination is to compute live burden appropriation factors (LLDFs) for inside and outside braces of on a level plane bended solid box support connects that have focal edges, inside one range surpassing 34 degrees. The geometry that is utilized in this investigation dependent on genuine geometry utilized in certain scaffolds. The objective of utilizing genuine geometry in this examination is to acquire progressively sensible, exact, and common sense outcomes. These outcomes will give factors that can be utilized by building planners to decide live burden conveyance factors on any individual required brace on a level plane bended solid box support spans. All straight and bended extensions that utilized in this investigation are kaleidoscopic in traverse the inside help.

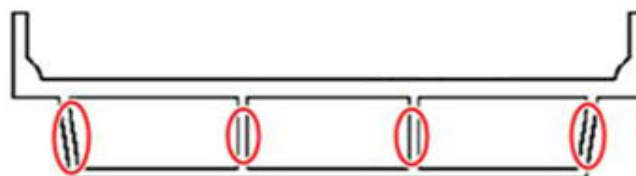


Figure 1.1: Interior and Exterior Girders that Carry the Design Vehicular Loads

## CURVED BRIDGES

Curved composite bridges have their unique characteristics. The curvature affects the geometry and behavior of the bridge structure. Curved bridges are subjected to coupled torsion and bending because of curvature and hence their analysis is more complex than that of straight bridges. In addition to simple vertical flexure behavior there can be significant torsional loading and twisting of the girders that cause lateral stresses to the flanges. Due to the complexity of the curved structure and its complicated 3D response different methods have been developed for the static and dynamic analysis of curved bridges. But now a day's 3D computer analysis is recommended for the analysis of horizontally curved bridges.

## FINITE ELEMENT METHOD

During the last two decades, the Finite Element Method (FEM) has become a popular technique in engineering for computerized complex solutions. The FEM solves the problem by using mathematical modeling in which the

structure should be considered as assembly of two or three dimensional elements connected to each other at their nodal points, possessing an appropriate number of degrees of freedom. The entire structure (Box Girder) is divided into small elements and the stiffness of that structure is assembled from the membrane and the plate bending stiffness of each element (Khairmode A. S. and Kulkarni D. B., 2016).

**LITERATURE REVIEW**

Bridge engineers have used the concept of distribution factors to estimate the transverse distribution of live loads since the 1930's. The live load distribution for moment and shear is essential to the design of new bridges and to evaluate the load carrying capacity of existing bridges. Big efforts have been made to develop and simplify the live load distribution equations. Also, many researches have been conducted in order to determine the effect of certain parameters, such as girder spacing, span length, and skew angle. The literature review presented in this chapter summarizes past findings that are relevant to this project and will only cover the following areas: background about previous AASHTO specification and AASHTO LRFD, summary of relevant research studies, AASHTO LRFD development, and current AASHTO formulas for box Girder Bridge

**2. DESCRIPTION OF MODEL BRIDGE AND LIVE LOADING**

For modeling and analyzing straight and curved bridges, some geometry are kept constant such as total deck width, number of cells (3 cells), left and right overhang, concrete strength and the girder spacing. The other geometry and properties, on the other hand, are different depending on the span length.

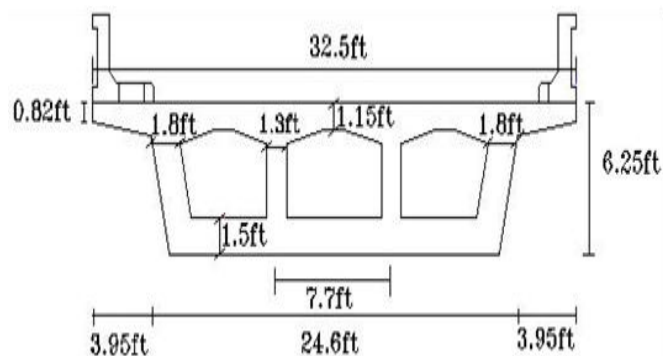


Figure 2 : Real Geometry of the Box Girder for Span Length of 115 ft.

3-D modeling analyses with shell element approach have been considered to model the concrete box-girder bridge as recommended by CSiBridge software program [12] and several researches [14]. Each shell element is a four-node area object used to model the entire bridge (superstructure and substructure). The superstructure and substructure of the box girder bridge is connected through link elements; each link has six degrees of freedom.

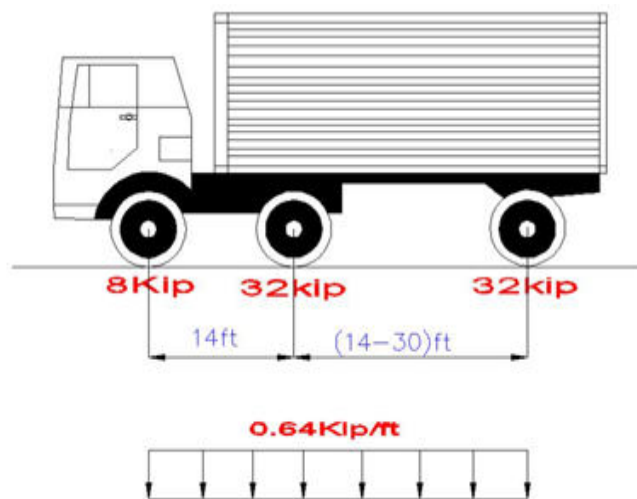


Figure 2: For the Maximum Positive Bending Moment Effect

For the all four cases mentioned, the distribution factors were calculated by loading the deck model with truck loads positioned at the longitudinal location that produces the maximum moment. The trucks were then moved transversely across the width of the bridge, and for each location the maximum girder moment was calculated, Figs 3.10. The largest girder (web) moment for all locations and load combinations was then selected as the maximum moment. This procedure was repeated for one and two number of design lanes that fit on the bridge transversely

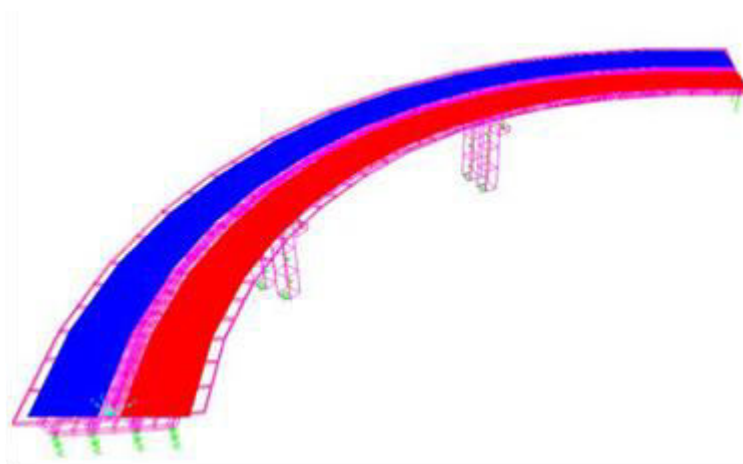
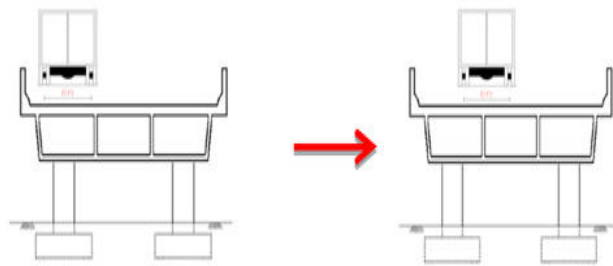


Figure 3: Both Lanes Loaded

The maximum one or two lane moment is caused either by a single design lane or two (or more) design lanes. The analysis involves the determination of the load in one and two lanes and load distribution to girders. The effect of multiple design lanes is determined by superposition. The maximum effects are calculated as the largest of the following cases:

Number of Loaded Lanes	Multiple Presence Factors “m”
1	1.20
2	1.00
3	0.85
>3	0.65

Table 1: Multiple Presence Factors



3-D modeling analyses have been conducted for straight bridges, Fig 4.1, for different span lengths (80, 90, 100, 115, 120, and 140 ft) and then the results compared with AASHTO LRFD, 2012 equations. This will help to get an indication and conception about the LLDF obtained from AASHTO LRFD formulas, 2012 to those obtained from finite element analyses for this type of bridge (Concrete Box Girder). Table 4.6.2.2.2b-1 and 4.6.2.2.2d-1, from AASHTO LRFD, 2012 [1] were used to calculate the LLDF for both interior and exterior girders, typical cross section (d) for Cast-in- Place Concrete Multi-cell Box, Fig 1.1. CSiBridge 2015, finite element analysis software program is being used to conduct 3-D modeling

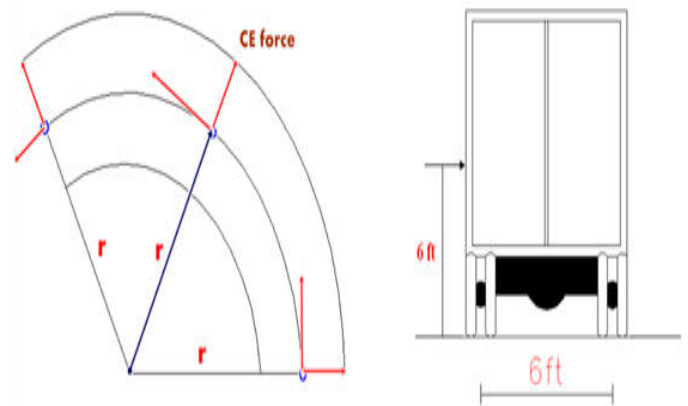
**4. Positive and Negative Moments (HL-93K)**

A single design truck combined with a design line load is typically used to determine the maximum positive moments. The back to back truck placement with 50 ft spacing (HL-93S in this thesis) normally controls for negative moment regions in bridges with long spans as those being studied in this research. However, a single truck must also be checked to see if it governs design of negative moment regions. First, the LLDF is determined for one lane loaded due to maximum positive and negative moments effect, Table 4.3 and 4.4. Then the LLDF is calculated for two lanes loaded under the maximum positive and negative moments Maximum Negative MomentLLDF for the negative bending moment in both exterior and interior girders for a one design lane loaded case.

About 35% is the percentage difference between the LLDF results that obtained from the analysis and AASHTO LRFD formula for interior girder, Fig 4.9 and about 37.5% in exterior girders as shown in Fig 4.10. For two lanes loaded, the percentage difference is 14% for interior girders,. With that lowest difference among the other load cases, the LLDF for the maximum negative bending moment for a single truck load (HL-93K) represents the largest bending moment of the all loading

**6. Comparison of the Results for Straight Bridges**

The Ccomparison between LLDF obtained from AASHTO LRFD, 2012 [1] to those obtained from finite element analyses are shown in Figures 4.4–4.6 for HL-93S and in Figs 4.7-4.12 for HL-93K loading type. AASHTO LRFD provides formulas to determine live load distribution factors for several common bridge superstructure types. However, there is a restriction of using these equations for curved bridges having central angles that exceed 34 degrees. Chapter 5 provides a study and modeling analyses for horizontally curved concrete box girder bridges that have a degree of curvature greater that 34 degree



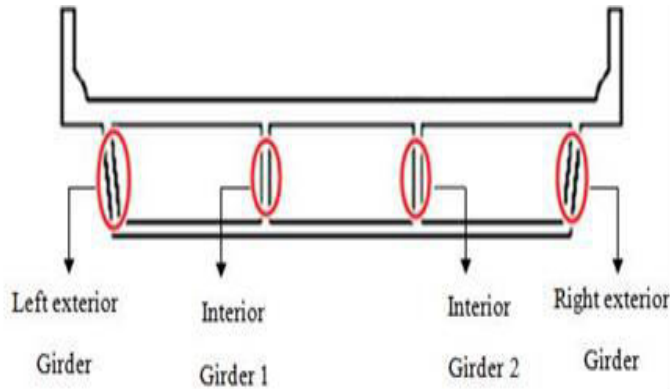
Braking Force, BR

The braking force shall be taken as the greatest of 25 percent of the axle weights of the design truck or five percent (5%) of the design truck plus lane load [1]. This braking force shall be placed in all design lanes which are considered to be loaded in accordance with Article 3.6.1.1.1 and which is carrying traffic headed in the same direction. These forces shall be assumed to act horizontally at a distance of 6.0 ft above the road way surface in either longitudinal direction to cause extreme force effects,

**7. RESULTS OF MOMENTS**

Tables A.1-A.6 show the results of maximum moments due to trucks HL-93K and HL-93S for straight bridges for each individual case. Tables A.7-A.12 state the moment results for curved bridges for different span lengths and central angles. These results represent the greatest negative moments that

occurred due to HL-93K, two lanes loaded, and for interior girder 1 (Fig A.1). Tables A.13-A.17 indicate the results of maximum moments for curved bridges that included the effects of centrifugal and braking forces. These values resulted in the highest LLDF for negative moment generated by the HL-93K loading, two lanes loaded, and for left exterior girder (Fig A.1), as the greatest moment occurs on the exterior girder as a results of the effect of centrifugal force.



3. CONCLUSIONS

Span Length (ft)	Entire Bridge	Interior Girder (1)	Interior Girder (2)	Left Exterior Girder	Right Exterior Girder
80	1998	600	655	320	591
90	2367	685	760	405	694
100	2738	765	850	499	790
115	3321	855	998	641	925
120	3525	915	1035	701	980
140	4376	1110	1240	908	1179

Table A.1: Results of Negative Moments (Kips-ft) for HL-93S- One Lane Loaded

Although the distribution factor formulas in AASHTO LRFD are considered to be more accurate than the distribution factors in the Standard Specifications, some researchers like Chen and Aswad, have found that they are conservative, and they are uneconomical for bridges with large span –to- depth ratios. According to Chen and Aswad the conservatism of the distribution factors can be 18 to 23 percent for interior girders and 4 to 12 percent for exterior girders [4].

LRFD Article 4.6.2.2.2 presents live load distribution factor formulas for several common types of bridge superstructures. These distribution factors provide a fraction of design lanes that should be used to an individual girder to design it for moment or shear. The factors take into account interaction among loads from multiple lanes. Table 1.1 shows some types of bridge superstructures with equations of live-load distribution factors for moment in interior and exterior girders for different types of straight bridges. There are many other types of bridge superstructures listed in the AASHTO LRFD [1].

REFERENCES

- Baldonado, M., Chang, C.-C.K., Gravano, L., Paepcke, A.: The Stanford Digital Library Metadata Architecture. Int. J. Digit. Libr. 1 (1997) 108–121
- Bruce, K.B., Cardelli, L., Pierce, B.C.: Comparing Object Encodings. In: Abadi, M., Ito, T. (eds.): Theoretical Aspects of Computer Software. Lecture Notes in Computer Science, Vol. 1281. Springer-Verlag, BerlinHeidelbergNew York (1997) 415–438
- van Leeuwen, J. (ed.): Computer Science Today. Recent Trends and Developments. Lecture Notes in Computer Science, Vol. 1000. Springer-Verlag, BerlinHeidelbergNew York (1995)
- Michalewicz, Z.: Genetic Algorithms + Data Structures = Evolution Programs. 3rd edn. Springer-Verlag, BerlinHeidelbergNew York (1996)1
- Acuña J, Palm B, Khodabandeh R, Weber K, 2010. Distributed temperature measurements on a U-pipe thermosyphon borehole heat exchanger with CO2. In 9th Gustav Lorentzen Conference on Natural Working Fluids Sydney, Australia. []
- Antonijevic D, Komatina M, 2011. Sustainable sub-geothermal heat pump heating in Serbia. Renewable and Sustainable Energy Reviews, 15(8), 3534–3538. []
- ASHRAE, 2016. ANSI/ASHRAE Standard 34–2016, Designation and Safety Classification of Refrigerants. ASHRAE, Atlanta. [Google Scholar]
- Austin BT, Sumathy K, 2011. Parametric study on the performance of a direct-expansion geothermal heat pump using carbon dioxide. Applied Thermal Engineering, 31(17), 3774–3782. []
- Bamigbetan O, Eikevik TM, Nekså P, Bantle M, 2017. Review of Vapour Compression Heat Pumps for High Temperature Heating using Natural Working Fluids. International Journal of Refrigeration. []
- Bolaji BO, Huan Z, 2013. Ozone depletion and global warming: Case for the use of natural refrigerant-a review. Renewable and Sustainable Energy Reviews, 18, 49–54. []
- Brignoli R, Brown SJ, Skye HM, Domanski PA, 2017. Refrigerant performance evaluation including effects of transport properties and optimized heat exchangers. International Journal of

- Refrigeration, 80, 52–65. [PMC free article] [PubMed] [Google Scholar]
- 8) Chargui R, Sammouda H, Farhat A, 2012. Geothermal heat pump in heating mode: and simulation on TRNSYS. International Journal of Refrigeration, 35(7), 1824–1832. [Google Scholar]
- 9) Cho HH, Domanski PA Optimized air-to-refrigerant heat exchanger with low-GWP refrigerants. 12th IIR Gustav Lorentzen Natural Working Fluids Conference, Edinburgh, 2016. [Google Scholar]
- 10) Choi J, Kang B, Cho H, 2014. Performance comparison between R22 and R744 solar-geothermal hybrid heat pumps according to heat source conditions. Renewable Energy, 71, 414–424. [Google Scholar]
- 11) Corberan JM, Finn DP, Montagud CM, Murphy FT, Edwards KC, 2011. A quasi-steady state mathematical model of an integrated ground source heat pump for building space control. Energy and Buildings, 43(1), 82–92. [Google Scholar]
- 12) Ebeling JC, Kabelac S, Luckmann S, Kruse H, 2017. Simulation and experimental validation of a 400 m vertical CO<sub>2</sub> heat pipe for geothermal application. Heat and Mass Transfer, 53, 3257–3265. [Google Scholar]
- 13) EIA, 2017. Monthly Energy Review. <https://www.eia.gov/totalenergy/data/monthly/>.
- 14) Eslami-Nejad P, Ouzzane M, Aidoun Z, 2014. Modeling of a two-phase CO<sub>2</sub>-filled vertical borehole for geothermal heat pump applications. Applied Energy, 114, 611–620. [Google Scholar]
- 15) Eslami-Nejad P, Ouzzane M, Aidoun Z, 2015. A quasi-transient model of a transcritical carbon dioxide direct-expansion ground source heat pump for space and water heating. Applied Thermal Engineering, 91, 259–269. [Google Scholar]

## BIOGRAPHIES

Mandeep Hooda, P.G Student, ,  
Matu Ram Institute of Engineering  
and Management, Rohtak, Haryana